IEEE Access
Multidisciplinary | Rapid Review | Open Access Journal

Received June 15, 2019, accepted June 26, 2019, date of publication July 5, 2019, date of current version July 25, 2019.

Digital Object Identifier 10.1109/ACCESS.2019.2927024

Frequency Constrained Optimal Siting and Sizing of Energy Storage

SHUCHANG YAN[1], (Student Member, IEEE), YU ZHENG[1,2], (Member, IEEE), AND DAVID JOHN HILL[1], (Fellow, IEEE)

[1]Department of Electrical and Electronic Engineering, The University of Hong Kong, Hong Kong
[2]School of Electrical and Information, Changsha University of Science and Technology, Changsha 410114, China

Corresponding author: Yu Zheng (zhy9639@hotmail.com)

This work was supported in part by the Hong Kong RGC Theme-Based Research Scheme under Project T23-701/12N and Project T23-701/14N, in part by the National Natural Science Foundation of China under Grant 71801021, and in part by the Training Program of the Major Research Plan of the National Natural Science Foundation of China under Grant 91746118.

ABSTRACT Frequency problem happens more frequently considering the current low-inertia system and the increasingly uncertain renewable energy sources. Energy storage is expected to provide the power with high ramping to reduce the power imbalance, and further, to maintain system frequency within an allowable range. In this paper, a framework for the planning of energy storage considering frequency constraints is proposed. The RoCoF and frequency nadir are constrained in this model, and reformulation linearization technique is utilized to relax the nonlinear constraints into linear constraints. Through this framework, optimal locations and the corresponding capacities of energy storage can be obtained. Case studies are conducted on a six-bus system and the RTS-76 system, and the results show that frequency requirements are satisfied for both centralized and distributed deployment of energy storage. In addition, also, the results show that deploying energy storage distributed is more economical and has less wind power curtailment.

INDEX TERMS Energy storage planning, frequency control, mixed integer linear programming.

I. INTRODUCTION

The current power system is becoming a low-inertia system [1]. And the diminished reserve from conventional synchronous generators for frequency control and the decreased and changeful rotational inertia in the system make that power system is vulnerable to frequency problems. This will strongly challenge us that if traditional frequency control strategy (primary, secondary and tertiary frequency control) can handle the frequency deviations brought by the faults or contingencies. For instances, when there is a fault or contingency, it is crucial to know that if the total exsiting rotational inertia and the reserve from power sources is sufficient to ensure the rate change of frequency (RoCoF) and frequency nadir not to exceed the pre-scheduled value and trigger the under frequency load shedding relays. These challenges force us to consider the possibility to use other power sources besides synchronous generators to respond to frequency deviations. Energy storage can store excess energy when there is a power generation surplus and release energy when there is a power shortage in power system. Also, energy storage is generally assumed to have a high ramping, which can follow the fast-changing net load demand. And the research question is *how to locate and size energy storage can have lowest operation cost of power system and energy storage cost while meeting the system frequency constraints?*

For application of energy storage on the generation side and power system operater side, reference [2] finds that distributed deployment of energy storage can relieve transmission line overloads and reduce the operation cost of the whole power system to benefit the wind power integration. Reference [3] finds that privately owned large scale energy storage can reduce the transmission line congestion while ensuring itself profitable. Reference [4] analyzes how to size the energy storage to reduce the risk brought by wind power forecast. For energy storage application on the consumer side, reference [5] utilizes energy storage to implement demand response to minimize the electricity cost of consumers and increase the comfort of customers. The performace of aforementioned applications is all related to the location, size, high ramping rate, power capacity, energy capacity, control strategy and the affiliation of energy storage. And also,

The associate editor coordinating the review of this manuscript and approving it for publication was Khmaies Ouahada.

background information such as wind integration level, load level and online existing generators of the power system is also important for the performance of energy storage.

The major application of energy storage in power system is to participate in the unit commitment and economic dispatch, however, it is noted that energy storage does not reach its maximum power capacity nor energy capacity in most of time in a day. And thus, the remaining power capacity and energy capacity have a potential possibility that they can be utilized for the frequency control. There is one way reported in the literature for energy storage to respond to the frequency deviations: when there is a contingency such as the trip of an online largest synchronous generators, energy storage receives the signal at once and discharges all its available power to the power system to reduce the power mismatch. Reference [6] sets this control method of energy storage as a corrective action to respond to the possible line outages. And based on this control strategy, the framework of corrective security-constrained optimal power flow (CSCOPF) is built and the corresponding hybrid algorithm is proposed. In this reference, the frequency indices of power system are not considered and the framework can only calculate the optimal power flow in one time period after the faults happen. Reference [7] proposes a method to estimate the power output of synchronous generators when there is a contingency in the power system. This method takes the rotational inertia and damping of synchronous generators into account and the condition to ensure the frequency nadir within the limits is given. Reference [8] adopts the frequency constraints in reference [7] and assumes that the energy storage discharges all its power to the power system when there is a contingency. However, the location and capacity of energy storage are fixed and the deployment of energy storage is not considered.

There are also a few references focusing on the siting and sizing of energy storage to minimize energy storage cost and operation cost of conventional generators. Reference [9] develops a step-by-step method to site and size energy storage. This method includes three steps: selecting the most favourable locations for energy storage is the first step, the second step is to select the power capacity and energy capacity of energy storage and conducting an optimal power dispatch scheme for power system including energy storage is the last step. Reference [10] gives a framework to analyze how to simultaneously expand the power capacities of generators, and power and energy capacities of energy storage. Primary frequency control and $N-1$ criterion are considered in this reference. The energy storage discharges all its remaining power to the power system when there is a generator trip. In reference [9], frequency constraints are not considered and only primary freqeuncy control is considered and inertial frequency control is neglected. There is also a problem on the calculation of investment cost of energy storage in references [9], [10]. In these two references, the investment cost of energy storage is set to be proportional to the power capacity and energy capacity, which is based on the calendar life. If we install energy storage based on calendar life as the former two references, and then energy storage will suffer from the problem of frequent charge and discharge in the operation, and finally energy storage will be scrapped much earlier than it is expected. Due to the fact that energy storage will undertake more tasks such as frequency control and load supplement in power system, the lifetime of energy storage such as batteries is more strictly limited by the total life cycles. It is noted that references [11]–[13] utilizes the similar cost functions to deploy energy storage.

Based on the literature review above, authors proposes a framework for power system operator to do the planning work of energy storage to acheive the lowest operation cost of power system and energy storage system cost. In this framework, the location and size of energy storage will be optimally decided such that system frequency requirements are met during a contingency. And the primary reserve of generators is also considered to ensure that frequency nadir is above the allowable value. The contributions of our work are as follows,

- We first give the mathematical formulation for energy storage planning where energy storage system cost is based on cycle life. This calculation method is more in line with practical engineering application.
- Frequency nadir and RoCoF, two key frequency evaluation metrics, are constrained in the mathematical model. This model is of great assistance for power system operator to reveal the value of energy storage by optimally choosing the location and size of energy storage to benefit the frequency security of current power system with high renewable energy sources.
- The location, size and physical characteristics of energy storage can be adjusted, and wind power can be curtailed. It is convenient for power system operator to study how these factors influence each other and how these factors interact with frequency constraints of power system.

II. LIFE CYCLE COST AND FREQUENCY CONTROL OF STORAGE

In this section, life cycle cost, frequency control strategy of storage and frequency model of power system will be introduced respectively.

A. LIFE CYCLE COST OF STORAGE

In this work, the types of energy storage to be installed are batteries such as lithium-ion batteries and lead-acid batteries, because they can be stacked up to provide desired energy capacity and power capacity based on specific requirements of technical applications and enviromental scenarios.

The total equivalent cycling life of lithium-ion and lead-acid batteries will remain stable if the depth of discharge is within pre-defined range [16]. In other words, the lifetime of batteries is calculated based on the cycle life, measured by the total energy usage. The battery storage cost is expressed

as follows [14],

$$C_B = C_I - C_R + C_O + C_M \tag{1}$$

where C_B is the total cost of energy storage, and it includes four parts: C_I is the investment cost corresponding to the total number of full equivalent cycles or total possible energy usage of batteries in their lifetime; C_R is the residual value, and it represents the number of unused full equivalent cycles or the amount of unused energy of batteries; C_o is the operation cost and C_M is the maintainance cost of batteries. If the lifetime measured by full equivalent cycles of all installed batteries will spend their all lifetime in practical use ($C_R = 0$), and then the total cost proportional to the energy capacity (USD/kWh) of batteries can be transformed to the costs measured by energy usage (per kWh) in the real operation. And it is represented as follows [15],

$$C_{B,i}(PB_{i,t}) = \lambda_{fix,i}\Delta t + \lambda_{cd,i}(1+\gamma_i)PB_{i,t}\Delta t \tag{2}$$

$$PB_{i,t} = PB_{i,t}^{cha} + PB_{i,t}^{dis} \tag{3}$$

where $C_{B,i}(PB_{i,t})$ (USD) is the cost related to battery at bus i at time t; $\lambda_{fix,i}$ is the fixed operation cost of battery storage at bus i in each hour (USD/h), which covers the investment cost of devices such as inverters and other hardwares, the operation cost C_O in (1) and the maintainance cost C_M in (1); $\lambda_{cd,i}$ is the charging/discharging cost (USD/kWh) of battery storage at bus i; $\lambda_{cd,i}(1+\gamma_i)PB_{i,t}\Delta t$ covers the difference value between the investment cost C_I and residue value C_R in (1), and it can be calculated through dividing the battery cost (USD/kWh) by total energy charging/discharging capability (kWh) in the whole cycle life of the certain type of batteries; $PB_{i,t}$ is the charged power $PB_{i,t}^{cha}$ or discharged power $PB_{i,t}^{dis}$ of battery at bus i at time t; γ_i is a loss coefficient of battery i, which stems from the charging and discharging efficiencies; Δt is the time interval duration between two neighbor time instances, and the time interval duration is 1 hour in this work.

B. FREQUENCY CONTROL OF STORAGE

The response time of batteries to control their charged or discharged power from zero to the power capacity is typically only hundreds of milliseconds. This high ramping capability will make that batteries can provide the immediate power support to the system and participate in frequency control. The control strategy of batteries following a contingency in power system is shown in Fig. 1. This strategy is divided into three stages.

1) When a contingency such as the trip of a generator happens, each battery will discharge all its available additional power to reduce the power imbalance in the system. This process is expressed by

$$\Delta PB_{i,t} = PB_{i,t}^{dis,max} - PB_{i,t}^{dis} + PB_{i,t}^{cha} \tag{4}$$

where $\Delta PB_{i,t}$ (MW) is the available additional power output of battery at bus i at time t, $PB_{i,t}^{dis}$ (MW) is the discharged power of battery at bus i at time t, $PB_{i,t}^{cha}$ (MW) is the charged power of battery at time i at time t, and one of them is zero due to the fact that battery can not charge power and discharge power simultaneously. Then the power shortage when all batteries provide available additional power is given as follows,

$$\Delta PM_t' = \Delta PM_t^{max} - \sum_{i}^{N} \Delta PB_{i,t} \tag{5}$$

where $\Delta PM_t'$ (MW) is the power shortage in power system when all the energy storage has discharged the remaining power to respond to the contingency, ΔPM_t^{max} (MW) is original power shortage caused by the contingency in power system. This stage corresponds to the inertial frequency control period, $\Delta t_1 = 5$s.

2) When frequency deviation in power system exceeds the governor dead band of generators, primary frequency control will be activated. In this stage, the discharged power of battery remains stable at the maximum discharged power. The time period is about 25s, $\Delta t_2 = 25$s.

3) After inertial and primary frequency response, frequency is at a value higher than the frequency nadir. And then, secondary frequency control will take effect to bring the frequency to the nomal value. At this time period, the discharged power of energy storage will come back linearly to 0. This time interval duration is about 5 min, $\Delta t_3 = 5$ min.

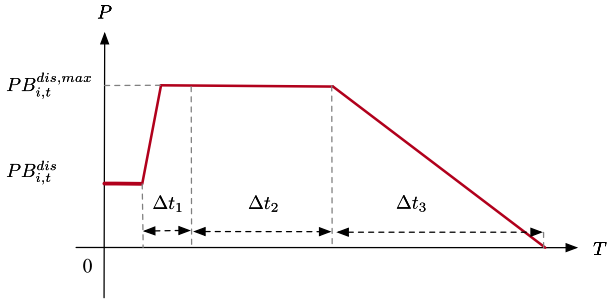

FIGURE 1. Control strategy of battery in a contingency.

To ensure that battery at bus i has enough energy to provide power support following a contingency at time t, part of energy should be reserved for this service. It can be calculated by

$$\Delta E_{i,t} = PB_{i,t}^{dis,max}(\Delta t_1 + \Delta t_2 + 0.5\Delta t_3) \tag{6}$$

where $\Delta E_{i,t}$ (MWh) is the maximum energy to be released of battery at bus i at time t, and Δt_1, Δt_2, Δt_3 are defined above. This equation calculates the maximum energy output of battery at bus i at time t when there is a contingency. We should limit

$$0 \le E_{i,t} - \Delta E_{i,t} \le E_i^{max} \tag{7}$$

where $E_{i,t}$ (MWh) is the stored energy of battery at bus i at time t. This constraint is to make sure that each energy storage has the energy reserve to respond to a contingency.

C. MODELING OF FREQUENCY DYNAMICS IN POWER SYSTEM

The swing equation for a single machine infinite bus system to represent the frequency dynamics is as follows,

$$M\frac{d\Delta f(t)}{dt} = \sum_{i=1}^{N}\Delta PB_i + \sum_{g=1}^{G}\Delta PG_g - \Delta PM \quad (8)$$

$$M = 2H \quad (9)$$

$$\Delta PG_g = -K_g(\Delta f(t) - f_g^{db}) \quad (10)$$

where G is the set of the synchronous generators in the power system, N is the set of buses in the power system, M is total inertia (MW·s/Hz), H is the total inertia constant (MW·s/Hz) in power system, ΔPM (MW) is power mismatch in power system, and this imbalance may come from the trip of a generator or a sudden increase of load, ΔPB_i (MW) is the additional available power output of battery at bus i when the contingency happens, $\Delta f(t)$ (Hz) is the frequency deviation in the power system, ΔPG_g (MW) is the automatic additional power output of synchronous generator indexed by g due to the droop control when frequency in power system changes, K_g (MW/Hz) is the droop coefficient of governor of generator indexed by g, and f_g^{db} is the dead band of the governor of generator indexed by g. Equation (8) shows that power imbalance results in frequency deviation in power system, and equation (10) shows that if frequency deviation exceeds the governor dead band of generator g, generator g will output power to reduce the power mismatch and counteract the further change of frequency. Frequency nadir is the point when frequency stops declining and starts to restore.

RoCoF and frequency nadir must be ensured to be within the pre-defined ranges to secure the frequency stability of power system.

III. PROBLEM FORMULATION

A. OBJECTIVE FUNCTION

The objective function is to minimize the sum of the operation cost of conventional generators and energy storage system cost in power system in a year. This leads to

$$C_{total} = \sum_{d=1}^{365}\sum_{t=1}^{24}\sum_{g=1}^{G}(C_{G,g}(PG_{g,t}) + ST_{g,t} + SD_{g,t} + c_g PR_{g,t}) + \sum_{d=1}^{365}\sum_{t=1}^{24}\sum_{i=1}^{N}C_{B,i}(PB_{i,t}) \quad (11)$$

where $C_{G,g}(PG_{g,t})$ (\$) is the operation cost of the synchronous generator g at time t in a quadratic form, $ST_{g,t}$ (\$) and $SD_{g,t}$ (\$) are the start-up and shut-down costs respectively of generator g at time t, $PR_{g,t}$ (MW) is the reserved power of generator g at time t and c_g (MW) is the cost coefficient for the reserve of generator g. The mathematical expression of $C_{G,g}(PG_{g,t})$, its corresponding linearization technique and the expression for the $ST_{g,t}$ and $SD_{g,t}$ can be found in references [17], [18]. The first four terms give the total cost related to the generators. The last term $C_{B,i}(PB_{i,t})$ is the cost of battery storage, which has been defined in (2).

B. CONSTRAINTS

1) CONSTRAINTS FOR NORMAL OPERATION

a: CONSTRAINTS OF BATTERY STORAGE

$$PB_{i,t}^{cha} = x_i\Upsilon_{i,t}^{cha} \quad (12)$$

$$PB_{i,t}^{dis} = x_i\Upsilon_{i,t}^{dis} \quad (13)$$

where x_i is the binary variable to represent whether there is battery storage at bus i. If x_i equals to 1, there exists battery storage at the bus i, and if x_i equals to 0, there is no battery storage at bus i; $\Upsilon_{i,t}^{cha}$ and $\Upsilon_{i,t}^{dis}$ are the fictitious variables representing the charged and discharged power when there is battery storage at bus i, and $PB_{i,t}^{cha}$ and $PB_{i,t}^{dis}$ are the real charged power and discharged power of battery storage at bus i at time t. These two constraints give the relationship between the locations of batteries and charged or discharged power of battery storage. It is noted that these two constraints are nonlinear due to multiplication of binary variables representing the locations of battery storage and decision variables representing fictitious charged and discharged power of battery storage, so they should be reformulated as follows,

$$0 \le PB_{i,t}^{cha} \le x_i \cdot M_1 \quad (14)$$

$$0 \le PB_{i,t}^{cha} - \Upsilon_{i,t}^{cha} \le M_1(1 - x_i) \quad (15)$$

$$0 \le PB_{i,t}^{dis} \le x_i \cdot M_1 \quad (16)$$

$$0 \le PB_{i,t}^{dis} - \Upsilon_{i,t}^{dis} \le M_1(1 - x_i) \quad (17)$$

where M_1 is large value ($M_1 = 1 \times 10^5$), and this method is called Big-M method in the opeartion research [19].

We should also limit that the battery storage can not charge or discharge power at the same time, so another two constraints are added as follows.

$$PB_{i,t}^{cha} \le M_2(1 - z_{i,t}) \quad (18)$$

$$PB_{i,t}^{dis} \le M_2 z_{i,t} \quad (19)$$

where $z_{i,t}$ is the binary variable. If $z_{i,t}$ equals to 1, the battery storage at bus i at time t can only discharge power. If $z_{i,t}$ equals to 0, the battery storage at bus i at time t can only charge power. Big-M method is employed again and M_2 is also a large value ($M_2 = 1 \times 10^5$). Then

$$E_{i,m} = E_{i,1} + \sum_{t=1}^{m}(\eta_{in,i}PB_{i,t}^{cha} - \frac{1}{\eta_{out,i}}PB_{i,t}^{dis}), \quad m = 1, 2, \ldots, T \quad (20)$$

$$E_{i,m} \ge 0 \quad (21)$$

where $E_{i,1}$ (MWh) is the initial energy level, $\eta_{in,i}$ is the charging efficiency, $\eta_{out,i}$ is the discharging efficiency for battery storage at bus i, $E_{i,m}$ (MWh) is the energy level of battery storage at bus i at time m and T is the total time periods for the scheduling. Constraint (20) gives the relationship between energy and power of battery storage at bus i,

and constraint (21) limits that the energy level of battery storage should not be negative at any time period. Note

$$E_i^{max} = max(E_{i,m}), \quad m = 1, 2, \ldots, T \tag{22}$$

$$E_{i,1} = E_{i,T} = \frac{1}{2}E_i^{max} \tag{23}$$

where E_i^{max} (MWh) is the maximum energy level (or energy capacity) of battery storage at bus i during the total T scheduling time periods. And we limit that the initial energy level and final energy level of battery at bus i are equal to allow battery storage to have energy to charge or discharge power at the initial time period. The following two constraints are given to limit the total energy capacity and number of battery storage to be deployed respectively as follows,

$$\sum_{i=1}^{N} E_i^{max} \le E_{total} \tag{24}$$

$$\sum_{i=1}^{N} x_i = s \tag{25}$$

where s is the total number of locations for the deployment of battery storage and E_{total} is the maximum energy capacity of energy storage to be deployed. Note

$$PB_i^{max} = max(PB_{i,m}^{cha} + PB_{i,m}^{dis}), \quad m = 1, 2, \ldots, T \tag{26}$$

$$E_i^{max} = \rho_i PB_i^{max} \tag{27}$$

where PB_i^{max} (MW) is the maximum charged power or discharged power of battery storage at bus i, and it can also be seen as the power capacity of this battery storage, ρ_i (h) is the energy-to-power ratio of battery storage at bus i, and constraint (27) gives the relationship between energy capacity and power capacity of battery storage at bus i.

b: CONSTRAINTS OF CONVENTIONAL GENERATORS

$$y_{g,t}PG_{g,t}^{min} \le PG_{g,t} \le y_{g,t}PG_{g,t}^{max} \tag{28}$$

$$-RD_g \le PG_{g,t+1}^{max} - PG_{g,t}^{max} \le RU_g \tag{29}$$

where $y_{g,t}$ is binary variables and represents the on-off status of generator g at time t. If $y_{g,t}$ is equal to 1, it means generator g is online at time t. If $y_{g,t}$ is equal to 0, it means generator g is offline; RD_i (MW/h) and RU_i (MW/h) are the maximum downward and upward ramping limits of generator g. These two constraints describe the power output limit and ramping limit of generator g at time t.

There are also the minimum up and down time constraints for conventional generators which can be found in reference [17].

c: CONSTRAINT OF NODAL BALANCE

$$PG_{i,t} + (1 - cw_{i,t})PW_{i,t} + PB_{i,t}^{dis} - PB_{i,t}^{cha} = \sum_{j \in \Omega_i} B_{i,j}(\theta_{i,t} - \theta_{j,t}) + PD_{i,t} \tag{30}$$

where $PW_{i,t}$ (MW) is power output of wind farm at bus i at time t, $PD_{i,t}$ (MW) is the load demand at bus i at time t, $cw_{i,t}$ is the wind power curtail rate of wind farm at bus i at time t, and it ranges from 0 to 1, $\theta_{i,t}$ and $\theta_{j,t}$ are the angle values at bus i and bus j at time t respectively, Ω_i is set of adjacent buses of bus i, and $B_{i,j}$ (S) is the susceptance of transmission line from bus i to bus j. Constraint (30) is the DC power balance constraint at each bus.

d: CONSTRAINTS OF TRANSMISSION LINES

$$-L_{sm}^{max} \le B_{s,m}(\theta_{s,t} - \theta_{m,t}) \le L_{sm}^{max} \tag{31}$$

$$-\pi \le \theta_{s,t} \le \pi \tag{32}$$

where $B_{s,m}$ (S) is the susceptance of transmission line from bus s to bus m respectively, $\theta_{s,t}$ and $\theta_{m,t}$ are the angle values at bus s and bus m at time t respectively, and L_{sm}^{max} is the maximum allowable power flow in the transmission line from bus s to bus m. Constraint (31) is the maximum line flow constraint and constraint (32) is the angle limit at each bus respectively.

2) CONSTRAINTS FOR THE CONTINGENCY

Based on the $N-1$ criterion, we assume that one largest online synchronous generator may trip during the operation of power system, and then energy storage discharges all its available power to the system, as is described in equation (4) and equation (5).

a: RoCoF CONSTRAINT

$$H_{total,t} = \sum_{g}^{G} H_g \cdot y_{g,t} \tag{33}$$

$$RoCoF = \frac{d\Delta f}{dt} = \frac{\Delta PM_t'}{2H_{total,t}} \le RoCoF^{max} \tag{34}$$

where $H_{total,t}$ (MW·s/Hz) is the total inertia constant in power system at time t and H_g is the inertia constant of generator g. The total inertia constant at time t is the sum of the inertia constant provided by online synchronous generators at time t and we also denote $M_{total,t} = 2H_{total,t}$. Constraint (34) is to limit that the initial RoCoF following a contingency is not larger than the maximum allowable RoCoF denoted as $RoCoF^{max}$ (Hz/s). This inequality is obtained from the swing equation of power system [20]. Due to the fact that decision variables $y_{g,t}$ are in the denominator which is nonlinear, it is reformulated to make this constraint linear as follows,

$$H_{total,t} = \sum_{g}^{G} H_g \cdot y_{g,t} \ge \frac{\Delta PM_t'}{2RoCoF^{max}} \tag{35}$$

b: CONSTRAINT OF FREQUENCY NADIR

$$PR_{g,t} \le 2v_g \frac{M_{total,t}(f^0 - f^{min} - f^{db})}{\Delta PM_t'} \tag{36}$$

$$\sum_{g}^{G} PR_{g,t} \ge \Delta PM_t' \tag{37}$$

where the $PR_{g,t}$ (MW) is primary reserve power of generator g at time t, f^0 is the nominal frequency, f^{min} is the minimum allowable frequency deviation (or frequency nadir) and f^{db} is the governors' dead band. The first constraint is to set the upper limit of reserve power for primary frequency control of generator g, and v_g (MW/s) is the maximum ramping rate for governor of generator g and it is the inherent property of generators. The value of v_g should be obtained from observations in practice or calculated from simulation when there is a large disturbance in power system. Block diagram of generators for simulation is given in [21]. The second constraint gives the condition to secure that frequency nadir is above the pre-set value. The derivation of these two constraints can be found in reference [7].

c: CONSTRAINTS OF BATTERY STORAGE

Constraints (6) and (7).

d: CONSTRAINTS OF CONVENTIONAL GENERATORS

$$0 \le PR_{g,t} \le PR_g^{max} \tag{38}$$

$$PG_{g,t} + PR_{g,t} \le y_{g,t} PG_g^{max} \tag{39}$$

The first constraint is to limit that primary reserve of generator g should not exceed its preset maximum value. And the second constraint is to limit that the sum of the power output and reserved power of generator g should not exceed the maximum power limit PR_g^{max}.

It is noted that transmission line constraints are not included in the constraints for the contingency due to the fact that the transmission line can endure overload for some time within the emergency rating [22], and this time interval duration is much larger than that of inertial and primary frequency control of power system.

IV. SOLVING METHOD

In the last section, problem formulation described by the objective function and constraints is a mixed integer linear programming (MILP) problem except constraints (22), (26) and (36).

For constraints (22) and (26), the *max* operator is utilized to obtain the maximum energy capacity and the maximum power capacity of battery storage to be deployed at each bus in power system respectively. And this operator can be implemented in YALMIP [23].

For constraint (36), it is first reformulated as follows,

$$\begin{aligned} PR_{g,t}\Delta PM_t' &= PR_{g,t}\Delta PM_t^{max} - PR_{g,t}\sum_{i=1}^{N} PB_{i,t}^{dis,max} \\ &\quad + PR_{g,t}\sum_{i=1}^{N} PB_{i,t}^{dis} - PR_{g,t}\sum_{i=1}^{N} PB_{i,t}^{cha} \\ &\le 2v_g M_{total,t}(f^0 - f^{min} - f^{db}) \end{aligned} \tag{40}$$

It can be seen that the nonlinear terms in constraint (40) are the $PR_{g,t}\sum_{i=1}^{N} PB_{i,t}^{dis,max}$, $PR_{g,t}\sum_{i=1}^{N} PB_{i,t}^{dis}$ and $PR_{g,t}\sum_{i=1}^{N} PB_{i,t}^{cha}$ because they are the multiplication of decision variables. Fortunately, $PR_{g,t}$, $\sum_{i=1}^{N} PB_{i,t}^{dis,max}$, $\sum_{i=1}^{N} PB_{i,t}^{dis}$ and $\sum_{i=1}^{N} PB_{i,t}^{cha}$ are bounded terms. And thus, new variables are expected to replace the nonlinear terms in this constraint through the reformulation-linearization technique [8], [24], and details can be seen in Appendix. We utilize $C_{g,t}^M$, $C_{g,t}^D$ and $C_{g,t}^C$ to represent $PR_{g,t}\sum_{i=1}^{N} PB_{i,t}^{dis,max}$, $PR_{g,t}\sum_{i=1}^{N} PB_{i,t}^{dis}$ and $PR_{g,t}\sum_{i=1}^{N} PB_{i,t}^{cha}$ respectively, and then we obtain the following constraint, together with constraints (A11)-(A16) in Appendix:

$$\begin{aligned} PR_{g,t}\Delta PM_t' &= PR_{g,t}\Delta PM_t^{max} - C_{g,t}^M + C_{g,t}^D - C_{g,t}^C \\ &\le 2v_g M_{total,t}(f^0 - f^{min} - f^{db}) \end{aligned} \tag{41}$$

After the mathematical manipulation above, the model becomes a MILP problem except the constraint (22) and constraint (26), and it can be solved in YALMIP using GUROBI 8.0.1 MILP solver on MATLAB.

V. CASE STUDY

This section includes two subsections.

The first subsection will conduct a unit commitment and economic dispatch with battery storage on a typical day. In this case study, frequency constraints and different locations of battery storage will be considered. To make the model proposed in the last section clear, a small-size six-bus system is utilized as a testcase.

The second subsection will select the optimal locations and determine the corresponding capacities for energy storage on a modified IEEE RTS-79 system. Different locations of battery storage on the total cost will be compared and how frequency constraints influence the total cost will be analyzed. Additional analysis such as the influence of the wind integration level on the total costs will also be presented.

All the parameters of test systems, generators, battery storage and the frequency control diagram of generators are accessible in [21] and the unit for cost analysis is the United States dollar ($) for these two cases. The simulation is on the computer with Intel i5 6500 3.2 GHz processor, 1TB hard disk and 16GB RAM.

A. SIX-BUS SYSTEM

1) SYSTEM DESCRIPTION

Fig. 2 shows the topology of six-bus system. Generators $G1$, $G2$ and $G3$ are located at bus 1, bus 2 and bus 6 respectively. There are loads at bus 3, bus 4 and bus 5. There is also a wind farm at bus 3. The base power capacity for this six-bus system is 100MVA and the base frequency is 50Hz. The contingency for this small scale system is set as a sudden increase of load 65MW. The cycle life of battery storage is 10000 full equivalent cycles, energy installation cost is 200 ($/kWh) and the round-trip efficiency is 92%. These are the parameters of the lithiom iron phosphate battery storage (LFP) with best performance in 2016. The maximum energy capacity to be deployed is 80MWh. The energy-to-power ratios of all

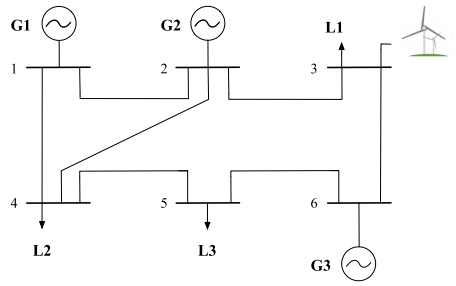

FIGURE 2. Six-bus system.

battery storage are 2 hours. The maximum allowable RoCoF is 0.62 Hz/s, the minimum allowable frequency deviation is set as the 49Hz and the governor's deadband is 20 mHz. In this case study, the following three cases will be analyzed:

- UCBF: Unit commitment and economic dispatch including battery storage is considered. And also, the RoCoF constraint and frequency nadir constraint are considered. The optimal locations are given by solution of model built in last section.
- UCB: Unit commitment and economic dispatch including battery storage is considered, however, the RoCoF constraint and frequency nadir constraint are not considered. The optimal locations are given by solution of model without frequency constraints.
- UCBF-C: Unit commitment and economic dispatch including battery storage is considered. And also, the RoCoF constraint and frequency nadir constraint are considered. We choose that the number of locations of battery storage equals to 1, and obtain only one optimal location of battery storage.

The load demand and wind power at each bus is shown in Fig. 3, and the MIP gap for GUROBI solver is 0.1%. Considering the low level integration of wind power, the wind curtailment is not implemented in six-bus system.

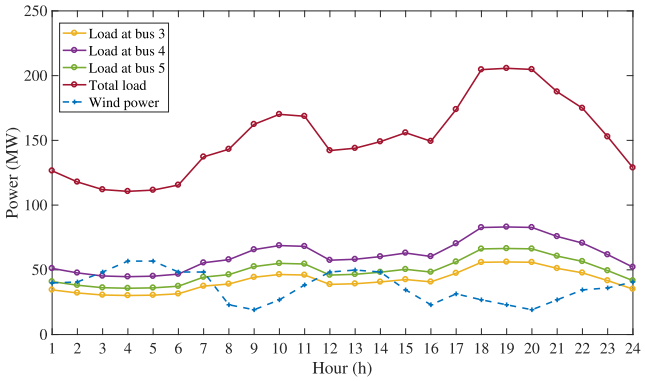

FIGURE 3. Load demand and wind power.

2) SIMULATION RESULTS

1. UCBF: Table 1 gives the best locations and the corresponding energy capacities of battery storage to be deployed.

TABLE 1. The locations and energy capacities for battery storage of UCBF.

Bus	1	2	3	4	5	6
Capacity (MWh)	37.2	5.36	17.27	10.65	9.52	0

Table 2 presents the on-off status of generators in power system at each hour in this typical day.

TABLE 2. Status of generators in a typical day of UCBF.

T	1	2	3	4	5	6	7	8	9	10	11	12	13	14
G1	1	1	1	1	1	1	1	1	1	1	1	1	1	1
G2	0	0	0	0	0	0	1	1	1	1	1	1	1	1
G3	1	1	1	0	1	1	1	1	1	1	1	1	1	1

T	15	16	17	18	19	20	21	22	23	24
G1	1	1	1	1	1	1	1	1	1	1
G2	1	1	1	1	1	1	1	1	1	1
G3	1	1	1	1	1	1	1	1	1	0

Fig. 4 presents the power output of conventional generators and charged or discharged power of battery storage in this typical day.

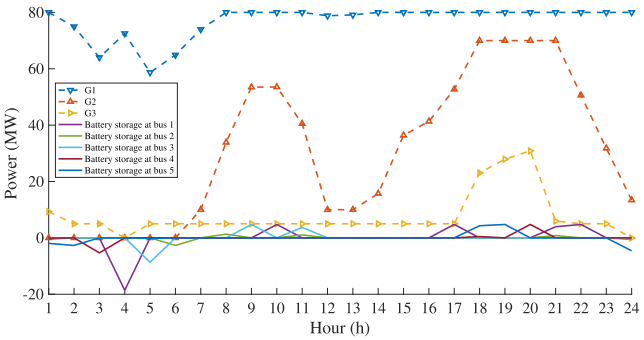

FIGURE 4. Power dispatch in a typical day of UCBF.

2. UCB: Table 3 gives the best locations and the corresponding energy capacities of battery storage to be deployed. Table 4 presents the on-off status of generators in power system at each hour in this typical day.

TABLE 3. The locations and energy capacities for battery storage of UCB.

Bus	1	2	3	4	5	6
Capacity (MWh)	24.28	19.50	0	0	6.86	29.36

Fig. 5 presents the power output of conventional generators and charged or discharged power of battery storage in this typical day.

3. UCBF-C: Table 5 gives the best locations and the corresponding energy capacities of battery storage to be deployed. Table 6 presents the on-off status of generators in power system at each hour in this typical day.

TABLE 4. Status of generators in a typical day of UCB.

T	1	2	3	4	5	6	7	8	9	10	11	12	13	14	15
G1	1	1	1	1	1	1	1	1	1	1	1	1	1	1	1
G2	0	0	0	0	0	0	1	1	1	1	1	1	1	1	1
G3	1	1	0	0	0	0	0	0	0	0	0	0	0	0	0

T	16	17	18	19	20	21	22	23	24
G1	1	1	1	1	1	1	1	1	1
G2	1	1	1	1	1	1	1	1	1
G3	0	0	1	1	1	1	0	0	0

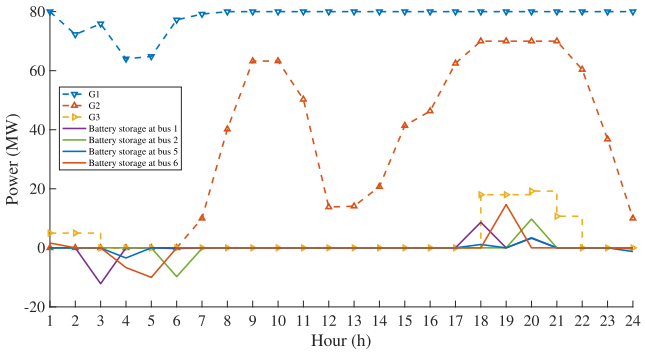

FIGURE 5. Power dispatch in a typical day of UCB.

TABLE 5. The locations and energy capacities for battery storage of UCBF-C.

Bus	1	2	3	4	5	6
Capacity (MWh)	0	0	0	80	0	0

TABLE 6. Status of generators in a typical day of UCBF-C.

T	1	2	3	4	5	6	7	8	9	10	11	12	13	14	15
G1	1	1	1	1	1	1	1	1	1	1	1	1	1	1	1
G2	1	1	0	0	0	0	1	1	1	1	1	1	1	1	1
G3	1	1	1	1	1	1	1	1	1	1	1	1	1	1	1

T	16	17	18	19	20	21	22	23	24
G1	1	1	1	1	1	1	1	1	1
G2	1	1	1	1	1	1	1	1	1
G3	1	1	1	1	1	1	1	1	0

Fig. 6 presents the power output of conventional generators and charged or discharged power of battery storage in this typical day.

3) ANALYSIS

In this typical day, there are two load peaks around from 9:00 to 12:00 and around from 18:00 to 21:00, and two load valleys around from 3:00 to 5:00 and around from 22:00 to 24:00. From the power dispatch scheme of UCB formulation in Fig. 5, battery storage at four buses all selects to charge power during the load valley around 3:00 to 5:00 and around 22:00 and 24:00, and discharges power during the load peak around 18:00 to 21:00. This is because this strategy of battery storage can take full advantage of cost difference of generators for the peak load and valley load and can reduce the totol cost including the operation cost of generators and battery storage cost to the greatest extent.

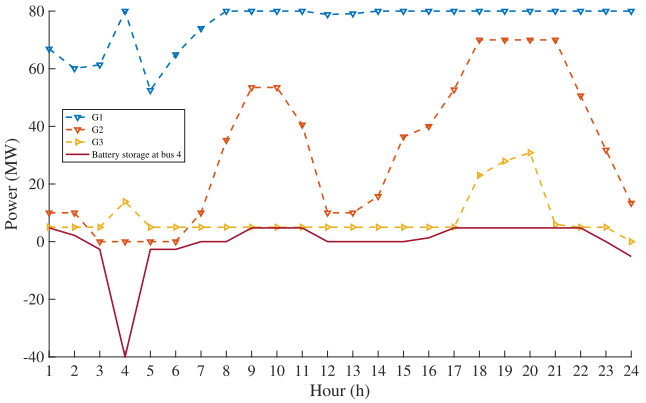

FIGURE 6. Power dispatch in a typical day of UCBF-C.

When RoCoF constraint and frequency nadir constraint are considered, as is described by the UCBF formulation, it can be seen from Fig. 4 that battery storage at the five buses chooses to charge power during the period of first load valley (3:00-5:00) and discharges power in both two load peak hours (9:00-12:00 and 18:00-21:00). This is due to the following reasons: during the second load peak hour, battery storage has the intention to minimize the total cost as well as to ensure frequency constraints of this system. And thus, battery storage can not discharge all the energy to the system during the second load peak hour, and reserve power is utilized to provide power support if a contingency happens due to the fact that the frequency constraints are hard constraints. After ensuring the frequency cosntraints, battery storage has to choose to discharge the power during the first peak load hours (9:00-12:00) to keep the initial and final stored energy at the same level and minimize the total cost.

The UCBF-C formulation considers the situation that battery storage is centralized deployed. The optimal location is bus 4 which has largest load in the system. Comparing Fig. 6 with Fig. 4, we can see that battery storage adopts the similar strategy to meet the frequency constraints and to reduce the total cost. The battery storage in the UCBF-C formulation delivers almost the same amount of power as that in the UCBF formualtion during the two load peak hours (9:00-12:00 and 18:00-21:00).

The on-off status of generators of different formulations (UCBF, UCB, UCBF-C) in this typical day are shown in Table 2, Table 4 and Table 6 respectively. We can see that generator G3 has to be online in most of the time in the UCBF formulation and UCBF-C formulation to contribute inertia and damping to meet the RoCoF and frequency nadir requirements of this six-bus system. And when the G3 is committed, it has to be operated at least with the minimum power output, which will increase the operation cost of generators.

Table 7 gives the value of objective functions in three cases; the unit for the cost is the United States dollar ($). CT represents the total cost of power system including the operation cost GO, the start-up cost GST, the shut-down cost GSD, the cost for the primary reserve GPR of synchronous generators, and battery storage cost CB. From Table 7, we can

TABLE 7. Cost comparisons of UCBF, UCB and UCBF-C.

Model	CT	GO	GST	GSD	GPR	CB
UCBF	48487	44953	100	50	2392.7	991.3
UCB	47502	44004	100	50	2393.1	954.9
UCBF-C	49155	45556	50	50	2451.8	1047.2

see that operation of power system based on the UCB formulation is the cheapest, the main function of generators is to meet load demand and provide the sufficient reserve power to meet the possible power shortage brought by the contingency. Operation of power system based on the UCBF formulation has the medium cost, because the RoCoF and frequency nadir should be ensured, which leads that additional conventional generators should be online and provide power to the system. Operation of power system based on the UCBF-C formulation has the highest cost and this can be seen that GO has increased by 1552 $ compared with that of UCB formulation. In fact, the net load demands considering the wind power have the different trends at different buses, that is, the load peaks and load valleys happen at different hours at different buses. And thus, battery storage in the way of centralized deployment can not fully grasp the opportunity to provide load leveling within the maximum line flow limits and angle limits.

Fig. 7 presents the RoCoF values of UCB, UCBF, and UCBF-C if power system experiences a contingency at each hour. It can be seen that the values of RoCoF under the UCB formulations are beyond the preset maximum allowable RoCoF value (0.62 Hz/s) most of the time in a day. And both UCBF and UCBF-C formulations can ensure that RoCoF is within the value of the maximum allowable RoCoF. However, there is no definite conclusion that which one can result in lower value of RoCoF in 24 hours of this typical day between UCBF and UCBF-C.

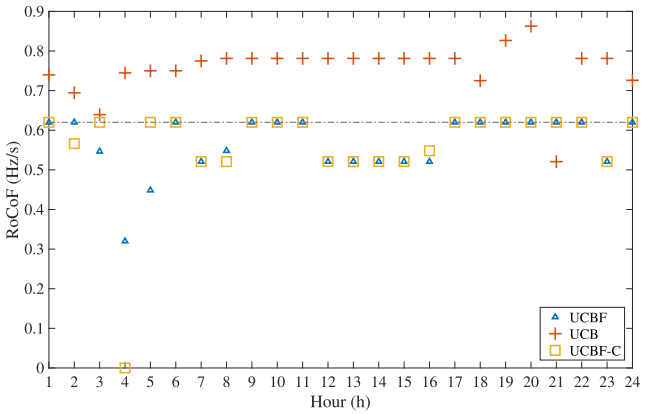

FIGURE 7. RoCoF of UCBF, UCB and UCBF-C.

B. IEEE RTS-76 SYSTEM

1) SYSTEM DESCRIPTION

The optimal deployment of battery storage will be conducted on the RTS-76 system in this section. RTS-76 system is well-known to be developed for reliability test and there are two benefits to employ this test system: first, relatively complete data can be found in this test system, and second, it is more convenient to compare the results from this work with ones from other researchers. RTS-76 system has 32 generation units at 10 buses of the total 24 buses. And also, the annual load profile on an hourly base can be obtained in reference [25]. The annual peak load is set as 3420 MW and the total installation capacity of generators is 5050MW in RTS-76 system. The topolgy of RTS-76 system is shown in Fig. 8. The line ratings of all transmission lines are set as 70% of the original value. Wind farms with total 1200MW capacity are installed in this system.

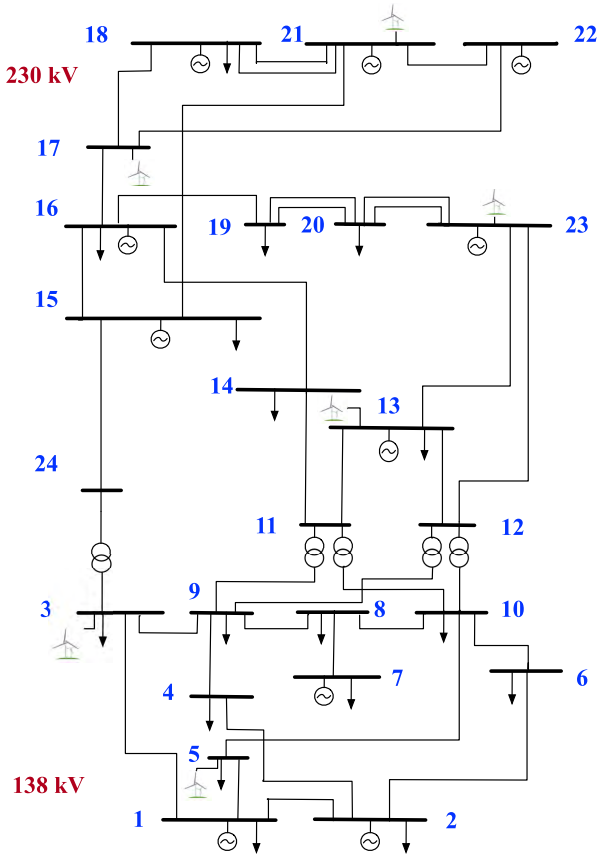

FIGURE 8. IEEE RTS-76 system.

And the locations of wind farms and the corresponding installation capacities are given in Table 8. The wind speed data with 10-minute interval for the year 2004 can be obtained from Western Wind Dataset on NREL's website [26]. The type of wind turbine in this system is Vetas V90 2MW, and its cut-in speed, rated speed and cut-out speed are 4 m/s, 12m/s and 25m/s respectively. The contingency of this system is the trip of the largest online nuclear power plant at bus 18. The maximum allowable RoCoF is 0.7 Hz/s, the minimum frequency nadir is 49.45Hz and the governor's deadband is 20 mHz. The maximum energy capacity of battery storage to be deployed is 200 MWh for this system. The MIP gap for the

TABLE 8. The locations and installation capacities of wind farms.

Bus	3	5	13	17	21	23
Capacity (MW)	150	200	250	100	150	50

GUROBI solver is 0.5%. Wind curtailment is implemented in this system. The LFP storage is selected as the potential battery storage, and the parameters representing the best performance of LFP in 2016 is adopted here. The relevant parameters are the same as these of six-bus system.

The total cost of centralized and distributed deployment of battery storage will be compared. The total cost of centralized deployment of battery storage is obtained by making that the total number of locations of battery storage equals to 1. The total cost of distributed deployment of battery storage is obtained by making that the total number of locations of battey storage equals to the number of buses in this system.

2) RESULTS AND ANALYSIS

For the centralized deployment of battery storage, the optimal location is bus 13 and the corresponding energy capacity is also 200MWh. And for the distributed deployment of battery storage, there are 8 buses to deploy battery storage and the total amount of energy capacities of battery storage is 200MWh. Optimal locations and the corresponding energy capacities are shown in Table 9.

TABLE 9. The locations and energy capacities for distributed deployment of battery storage.

Bus	2	5	14	15
Capacity (MWh)	24.4015	23.6292	18.6249	36.9961
Bus	16	17	18	21
Capacity (MWh)	38.8529	14.2205	8.7853	34.4896

The costs of centralized and distributed battery storage are shown in Table 10; GT is the cost of generators including the operation cost GO, start-up cost GST and shut-down cost GSD; GPR is the primary reserve cost of generators; CB is the installation cost of battery storage and CW is the total power of wind curtailment. It can be seen that in Table 10 that distributed deployment of battery storage can significantly reduce the operation cost of generators and the primary reserve cost. Also, the total wind power curtailment is also significantly reduced.

TABLE 10. Cost comparisons of centralized and distributed deployments of battery storage.

Model	GT ($)	GPR ($)	CB ($)	CW (MW)
Centralized	3.1039×10^8	8.7504×10^6	1.0458×10^6	2.0879×10^5
Distributed	3.0464×10^8	8.7462×10^6	1.4994×10^6	8.5749×10^3

Wind curtailment is caused by two reasons. One reason is that power output of wind farm should meet the angle and the maximum line flow limits of power system. If power output of wind farm is very large, it has to be curtailed to meet the network constraints. Another reason is that more expensive generators will be online at least with the minimum power output to provide inertia and primary reserve power to meet the frequency constraints, and this will decrease the transmission capacity of transmission lines for the wind power, and then reduce the allowable range of power output of wind farms. It also can be seen that the cost for the distributed deployment of battery storage is much higher than that for centralized deployment of battery storage, and this means that more utilization is for distributed deployment of battery storage rather than centralized deployment of battery storage.

We fix the locations and capacities of battery storage, and change the maximum allowable RoCoF from 0.64 Hz/s to 0.76 Hz/s and the minimum allowable frequency deviation from 49.5 Hz to 49.71 Hz respectively to see how these two pre-set parameters of frequency constraints influence the total costs of power system with centralized deployment of battery storage and distributed deployment of battery storage.

Fig. 9 and Fig. 10 show that how the total cost and curtailed wind power change with the maximum allowable RoCoF respectively. Total cost here includes the cost related to the generators, primary reserve cost and energy storage cost. It can be seen that total cost and curtailed wind power will both have significant increases when the value of the maximum allowable RoCoF decreases for both cases where the battery storage is centralized or distributed. However, the total cost and curtailed wind power with distributed deployment of battery storage are much lower than these with centralized deployment of battery storage. It also can be seen that when the maximum allowable RoCoF is in the range between 0.72 Hz/s and 0.76 Hz/s, the change rate of curtailed wind power are relatively slow, which means the influence of RoCoF constraint on the curtailed wind power decreases.

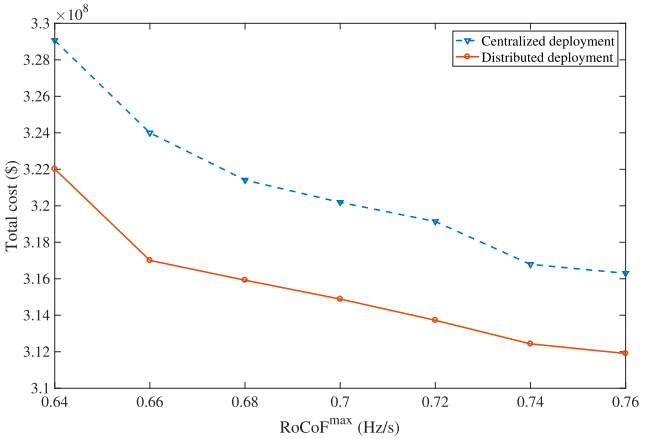

FIGURE 9. Total cost with the change of $RoCoF^{max}$.

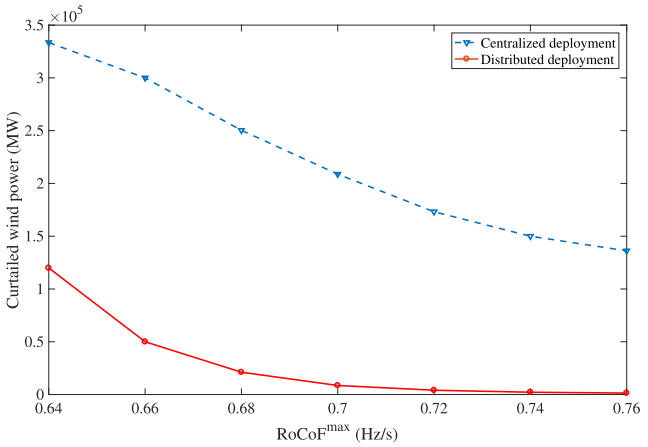

FIGURE 10. Curtailed wind power with the change of $RoCoF^{max}$.

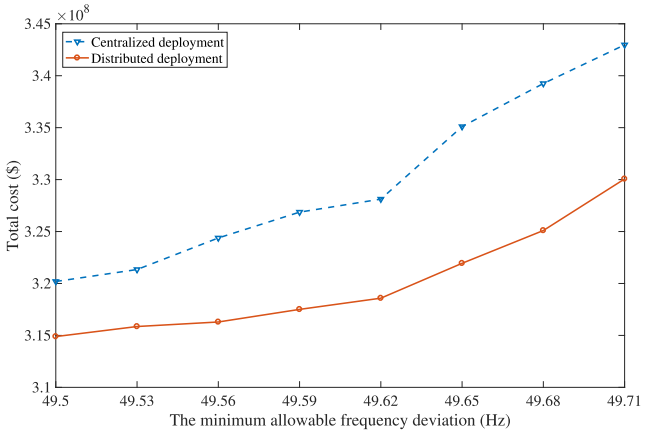

FIGURE 11. Total cost with the change of the minimum allowable frequency deviation.

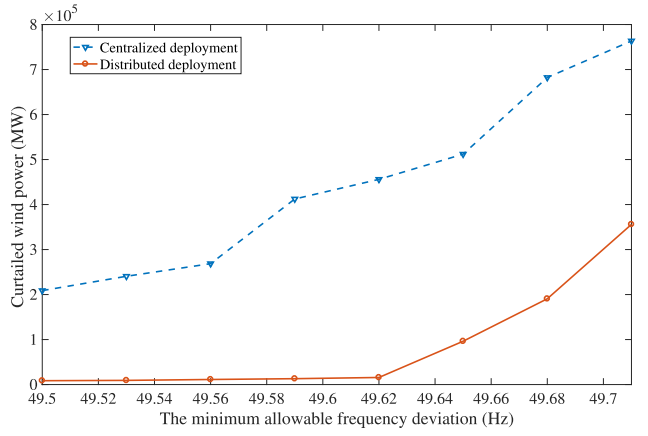

FIGURE 12. Curtailed wind power with the change of the minimum allowable frequency deviation.

Fig. 11 and Fig. 12 show that how the total cost and the curtailed wind power change with the minimum allowable frequency deviation respectively. It can be seen that total cost and curtailed wind power will have significant increases when the value of the minimum allowable frequency deviation increases for both cases where the battery storage is centralized or distributed. However, the total cost and curtailed wind power for distributed deployment of battery storage are also much lower than these with centralized deployment of battery storage. For the distributed deployment of battery storage, the change of total cost and curtailed wind power are much faster with the increase of the value of the minimum frequency deviation, which means that the influence of the minimum allowable frequency deviation constraint on the total cost of power system is enhanced.

From Fig. 9 to Fig. 12, we can see both RoCoF constraint and the minimum allowable frequency deviation constraint take effects. This is because that higher frequency requirement will make that battery storage reserves more power for the possible contingency, and the function of energy storage for load peak shaving and valley filling weakens, and thus, total cost and curtailed wind power increase. Compared with centralized deployment of battery storage, distributed deployment of battery storage will be less restricted by the network constraints and can take full advantage of the varying net load profiles at different buses, and thus, distributed deployment of battery storage can have lower total cost and curtailed wind power.

If locations of battery storage are fixed and total energy capacity of battery storage changes from 160 MWh to 240 MWh, the change of total cost with centralized deployment and distributed deployment of battery storage is shown in Fig. 13 and Fig. 14 respectively. We can see that for both the states, the total cost is decreased significantly. The reason is that battery storage with more energy capacity can better achieve peak shaving and load filling to bring down the operation cost of generators and reduce the need of primary reserve from synchronous generators. Wind power could be less curtailed so that the net load demand will be fewer, which reduces the operation cost of generators to meet the net load. And also, we still see that distributed deployment of battery storage enjoys a lower total cost compared with centralized deployment of battery storage.

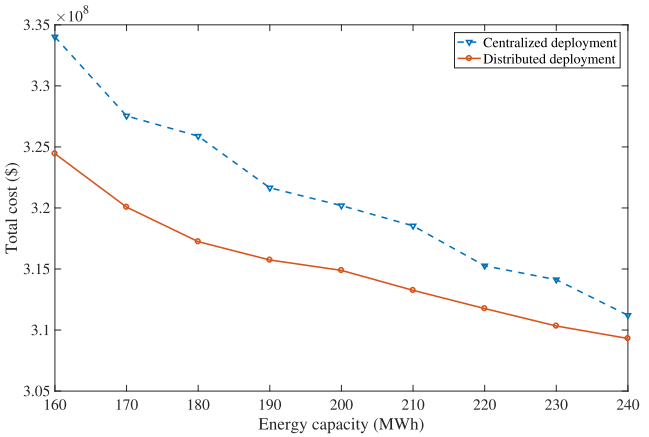

FIGURE 13. Total cost with change of energy capacity of battery storage.

Finally, wind integration level is changed by adjusting the total installation capacity of wind farms in this system.

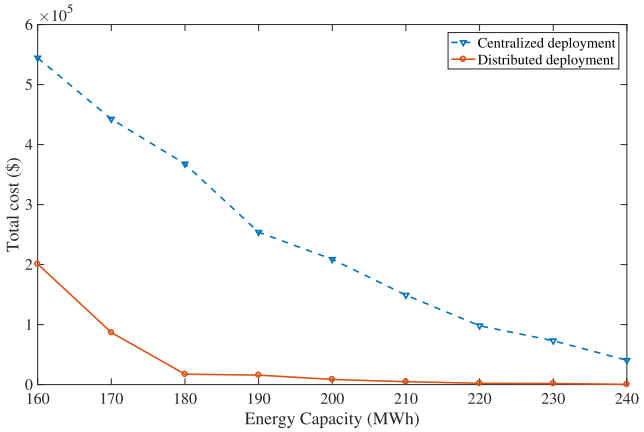

FIGURE 14. Curtailed wind power with change of energy capacity of battery storage.

The installation capacity of wind farms will increase from 600MW to 1200MW, and the newly added capacity is expanded proportionally to the original installation capacity of wind farm at each bus. Fig. 15 shows that the total costs both with centralized deployment and distributed deployment

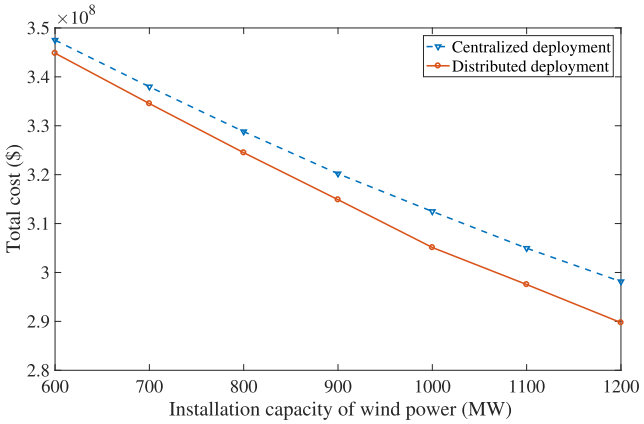

FIGURE 15. Total cost with change of wind integration level.

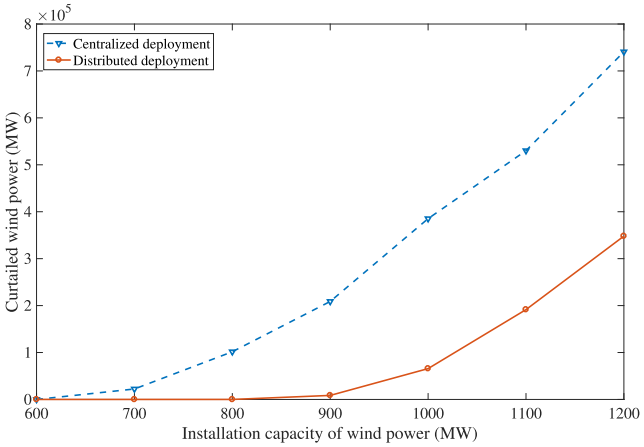

FIGURE 16. Curtailed wind power with change of wind integration level.

of battery storage will reduce to a great extent. This is because more integration of wind power will reduce the total net load, and less power output from synchronous generators are required. At each wind integration level, the total cost of distributed deployment of battery storage is lower than that of centralized deployment of battery storage. The curtailed wind power increases in both cases due to the fact that integration of wind power increases and more wind power should be curtailed to meet the network constraints, as is shown in Fig. 16.

VI. CONCLUSION

In our framework, energy storage engaged in power balance and frequency control of power system. Energy storage discharged all its remaining available power to the system when there was a power shortage. A mathematical model for the planning of energy storage considering frequency constraints was proposed, and the costs for centralized and distributed deployment of energy storage were compared. The major discoveries and contributions are listed as follows:

1) Raising the requirement of frequency indices including the RoCoF and frequency nadir will significantly increase the total cost of power system. The first reason is that more generators should be online at least with the minimum power output. The second reason is that the part of power capacity and energy capacity of battery storage reserved for frequency response will increase. The capability of energy storage engaging in the unit commitment and economic dispatch will be reduced. And thus, the curtailed wind power will increase and the need for new generators to be online grows. The last reason is that more reserve power is required from the synchronous generators, which will cause higher reserve cost and the incremental need for synchronous generators to be online. These factors interwine with each other, and finally total cost increases.

2) Both centralized and distributed deployments of battery storage can ensure the frequency requirement of power system. However, compared with the centralized deployment of energy storage, it is found that the distributed demployment of energy storage will have more benefits. Energy storage of distributed deployment can respond to the varying load profiles at different buses to a greater extent and can reduce the restriction of power flow constraints. And thus, the total cost of distributed deployment of energy storage will be much lower than that of centralized deployment of energy storage at different frequency requirements, energy capacities of energy storage and wind integration levels.

APPENDIX

Reformulation linearization method [8], [24] is utilized to relax nonlinear constraints. The detailed process is illustrated as follows,

i. The nonlinear terms $a_i b_i$ are the multiplcation of two decision variables a_i and b_i, and the corresponding lower and upper bound is known, $a_i^{min} \le a_i \le a_i^{max}$, $b_i^{min} \le b_i \le b_i^{max}$.

ii. Replace $a_i b_i$ with $C_{i,j}$, and obtain the following four constraints for the term $C_{i,j}$ in the optimization problem.

$$(a_i - a_i^{min})(b_j - b_j^{min}) \geq 0$$
$$\Rightarrow C_{i,j} - b_j^{min} a_i - a_i^{min} b_j + a_i^{min} b_j^{min} \geq 0 \quad \text{(A1)}$$
$$(a_i - a_i^{min})(b_j^{max} - b_j) \geq 0$$
$$\Rightarrow -C_{i,j} + b_j^{max} a_i - a_i^{min} b_j^{max} + a_i^{min} b_j \geq 0 \quad \text{(A2)}$$
$$(a_i^{max} - a_i)(b_j - b_j^{min}) \geq 0$$
$$\Rightarrow -C_{i,j} + a_i^{max} b_j - a_i^{max} b_j^{min} + b_j^{min} a_i \geq 0 \quad \text{(A3)}$$
$$(a_i^{max} - a_i)(b_j^{max} - b_j) \geq 0$$
$$\Rightarrow C_{i,j} + a_i^{max} b_i^{max} - a_i^{max} b_j - b_j^{max} a_i \geq 0 \quad \text{(A4)}$$

Based on the problem formulation, we first list the lower and upper limits of the decision variables as follows,

$$0 \leq PR_{g,t} \leq PR_g^{max} \quad \text{(A5)}$$
$$0 \leq \sum_{i=1}^{N} PB_{i,t}^{dis,max} = \sum_{i=1}^{N} \frac{E_i^{max}}{\rho_i} \leq \frac{E_{total}}{\min_{i=1,\ldots,N}(\rho_i)} \quad \text{(A6)}$$
$$0 \leq \sum_{i=1}^{N} PB_{i,t}^{dis} \leq \sum_{i=1}^{N} \frac{E_i^{max}}{\rho_i} \leq \frac{E_{total}}{\min_{i=1,\ldots,N}(\rho_i)} \quad \text{(A7)}$$
$$0 \leq \sum_{i=1}^{N} PB_{i,t}^{cha} \leq \sum_{i=1}^{N} \frac{E_i^{max}}{\rho_i} \leq \frac{E_{total}}{\min_{i=1,\ldots,N}(\rho_i)} \quad \text{(A8)}$$

There also exists inequalities as follows,

$$PR_{g,t} \sum_{i=1}^{N} PB_{i,t}^{dis} \leq PR_{g,t} \sum_{i=1}^{N} PB_{i,t}^{dis,max} \quad \text{(A9)}$$
$$PR_{g,t} \sum_{i=1}^{N} PB_{i,t}^{cha} \leq PR_{g,t} \sum_{i=1}^{N} PB_{i,t}^{dis,max} \quad \text{(A10)}$$

And then, we utilize $C_{g,t}^M$, $C_{g,t}^D$ and $C_{g,t}^C$ to represent $PR_{g,t} \sum_{i=1}^{N} PB_{i,t}^{dis,max}$, $PR_{g,t} \sum_{i=1}^{N} PB_{i,t}^{dis}$ and $PR_{g,t} \sum_{i=1}^{N} PB_{i,t}^{cha}$ respectively. Based on the (A1)-(A4) and (A9)-(A10), we can obtain the following constraints:

$$C_{g,t}^M \geq 0 \quad \text{(A11)}$$
$$-C_{g,t}^M + \frac{E_{total}}{\min_{i=1,\ldots,N}(\rho_i)} PR_{g,t} \geq 0 \quad \text{(A12)}$$
$$-C_{g,t}^M + PR_{g,t}^{max} \sum_{i=1}^{N} PB_{i,t}^{dis,max} \geq 0 \quad \text{(A13)}$$
$$C_{g,t}^M + PR_{g,t}^{max} \frac{E_{total}}{\min_{i=1,\ldots,N}(\rho_i)} - PR_{g,t}^{max} \sum_{i=1}^{N} PB_{i,t}^{dis,max} - PR_{g,t} \frac{E_{total}}{\min_{i=1,\ldots,N}(\rho_i)} \geq 0 \quad \text{(A14)}$$
$$0 \leq C_{g,t}^C \leq C_{g,t}^M \quad \text{(A15)}$$
$$0 \leq C_{g,t}^D \leq C_{g,t}^M \quad \text{(A16)}$$

REFERENCES

[1] A. Ulbig, T. S. Borsche, and G. Andersson, "Impact of low rotational inertia on power system stability and operation," 2013, *arXiv:1312.6435*. [Online]. Available: https://arxiv.org/abs/1312.6435

[2] M. Ghofrani, A. Arabali, M. Etezadi-Amoli, and M. S. Fadali, "A framework for optimal placement of energy storage units within a power system with high wind penetration," *IEEE Trans. Sustain. Energy*, vol. 4, no. 2, pp. 434–442, Apr. 2013.

[3] H. Khani, M. R. D. Zadeh, and A. H. Hajimiragha, "Transmission congestion relief using privately owned large-scale energy storage systems in a competitive electricity market," *IEEE Trans. Power Syst.*, vol. 31, no. 2, pp. 1449–1458, Mar. 2016.

[4] H. Bludszuweit and J. A. Domínguez-Navarro, "A probabilistic method for energy storage sizing based on wind power forecast uncertainty," *IEEE Trans. Power Syst.*, vol. 26, no. 3, pp. 1651–1658, Aug. 2011.

[5] V. Pradhan, V. S. K. Balijepalli, and S. A. Khaparde, "An effective model for demand response management systems of residential electricity consumers," *IEEE Syst. J.*, vol. 10, no. 2, pp. 434–445, Jun. 2016.

[6] J. Cao, W. Du, and H. F. Wang, "An improved corrective security constrained OPF with distributed energy storage," *IEEE Trans. Power Syst.*, vol. 31, no. 2, pp. 1537–1545, Mar. 2016.

[7] H. Chávez, R. Baldick, and S. Sharma, "Governor rate-constrained OPF for primary frequency control adequacy," *IEEE Trans. Power Syst.*, vol. 29, no. 3, pp. 1473–1480, May 2014.

[8] Y. Wen, W. Li, G. Huang, and X. Liu, "Frequency dynamics constrained unit commitment with battery energy storage," *IEEE Trans. Power Syst.*, vol. 31, no. 6, pp. 5115–5125, Nov. 2016.

[9] H. Pandžić, Y. Wang, T. Qiu, Y. Dvorkin, and D. S. Kirschen, "Near-optimal method for siting and sizing of distributed storage in a transmission network," *IEEE Trans. Power Syst.*, vol. 30, no. 5, pp. 2288–2300, Sep. 2015.

[10] M. Carrión, Y. Dvorkin, and H. Pandžić, "Primary frequency response in capacity expansion with energy storage," *IEEE Trans. Power Syst.*, vol. 33, no. 2, pp. 1824–1835, Mar. 2018.

[11] R. Fernández-Blanco, Y. Dvorkin, B. Xu, Y. Wang, and D. S. Kirschen, "Optimal energy storage siting and sizing: A WECC case study," *IEEE Trans. Sustain. Energy*, vol. 8, no. 2, pp. 733–743, Apr. 2017.

[12] B. Xu, Y. Wang, Y. Dvorkin, R. Fernández-Blanco, C. A. Silva-Monroy, J.-P. Watson, and D. S. Kirschen, "Scalable planning for energy storage in energy and reserve markets," *IEEE Trans. Power Syst.*, vol. 32, no. 6, pp. 4515–4527, Nov. 2017.

[13] Y. Dvorkin, "Can merchant demand response affect investments in merchant energy storage?" *IEEE Trans. Power Syst.*, vol. 33, no. 3, pp. 2671–2683, May 2018.

[14] Y. Zheng, Z. Y. Dong, F. J. Luo, K. Meng, J. Qiu, and K. P. Wong, "Optimal allocation of energy storage system for risk mitigation of DISCOs with high renewable penetrations," *IEEE Trans. Power Syst.*, vol. 29, no. 1, pp. 212–220, Jan. 2014.

[15] Y. Zheng, J. Zhao, Y. Song, F. Luo, K. Meng, J. Qiu, and D. J. Hill, "Optimal operation of battery energy storage system considering distribution system uncertainty," *IEEE Trans. Sustain. Energy*, vol. 9, no. 3, pp. 1051–1060, Jul. 2018.

[16] D. Linden and T. Reddy, *Handbook of Batteries*, vol. 4. New York, NY, USA: McGraw-Hill, 2002.

[17] M. Carrión and J. M. Arroyo, "A computationally efficient mixed-integer linear formulation for the thermal unit commitment problem," *IEEE Trans. Power Syst.*, vol. 21, no. 3, pp. 1371–1378, Aug. 2006.

[18] L. Wu, M. Shahidehpour, and T. Li, "Stochastic security-constrained unit commitment," *IEEE Trans. Power Syst.*, vol. 22, no. 2, pp. 800–811, May 2007.

[19] F. S. Hillier, *Introduction to Operations Research*. New York, NY, USA: McGraw-Hill, 2012.

[20] P. Kundur, N. J. Balu, and M. G. Lauby, *Power System Stability and Control*, vol. 7. New York, NY, USA: McGraw-Hill, 1994.

[21] S. Yan. *Data for Simulation*. Accessed: Jun. 7, 2019. [Online]. Available: https://pan.baidu.com/s/1yrgMIqdcnApARV8cRqyL1Q

[22] B. P. Bhattarai, J. P. Gentle, T. McJunkin, P. J. Hill, K. S. Myers, A. W. Abboud, R. Renwick, and D. Hengst, "Improvement of transmission line ampacity utilization by weather-based dynamic line rating," *IEEE Trans. Power Del.*, vol. 33, no. 4, pp. 1853–1863, Aug. 2018.

[23] J. Lofberg, "YALMIP: A toolbox for modeling and optimization in MATLAB," in *Proc. IEEE Int. Conf. Robot. Automat.*, Sep. 2004, pp. 284–289.

[24] H. D. Sherali and W. P. Adams, *A Reformulation-Linearization Technique for Solving Discrete and Continuous Nonconvex Problems*, vol. 31. New York, NY, USA: Springer, 2013.
[25] P. M. Subcommittee, "IEEE reliability test system," *IEEE Trans. Power App. Syst.*, vol. 98, no. 6, pp. 2047–2054, Nov. 1979.
[26] C. W. Potter, D. Lew, J. McCaa, S. Cheng, S. Eichelberger, and E. Grimit, "Creating the dataset for the western wind and solar integration study (USA)," *Wind Eng.*, vol. 32, no. 4, pp. 325–338, 2008.

SHUCHANG YAN (S'17) received the B.E. degree from North China Electric Power University, China. He is currently pursuing the M.Phil. degree with the Department of Electrical and Electronic Engineering, The University of Hong Kong.

His research interests include optimization theory, control theory, and their applications in energy storage systems in power systems.

YU ZHENG (M'15) received the B.E. degree from Shanghai Jiao Tong University, China, in 2009, and the Ph.D. degree from the University of Newcastle, Australia, in 2015. He is currently a Senior Research Assistant with The University of Hong Kong, Hong Kong. He is also a Visiting Professor with the Changsha University of Science and Technology, Changsha, China. His research interests include power electronic applied in power systems, power system planning, and smart grid.

DAVID JOHN HILL (S'72–M'76–SM'91–F'93–LF'14) received the B.E. degree in electrical engineering and the B.Sc. degree in mathematics from The University of Queensland, Australia, in 1972 and 1974, respectively, and the Ph.D. degree in electrical engineering from the University of Newcastle, Australia, in 1976. He holds the Chair of electrical engineering with the Department of Electrical and Electronic Engineering, The University of Hong Kong, where he directs the Centre for Electrical Energy Systems and also the Program Coordinator of the Multi-university RGC Theme-Based Research Scheme Project on Sustainable Power Delivery Structures for High Renewables. He is also a part-time Professor and the Director of the Centre for Future Energy Networks, The University of Sydney, Australia. From 2005 to 2010, he was an Australian Research Council Federation Fellow with The Australian National University. Since 2006, he has been the Theme Leader of Complex Networks and the Deputy Director of the ARC Centre of Excellence for Mathematics and Statistics of Complex Systems.

He has been holding various positions at The University of Sydney, since 1994, including the Chair of electrical engineering, until 2002 and from 2010 to 2013, along with an ARC Professorial Fellowship. He has also held academic and substantial visiting positions at The University of Melbourne; the University of California at Berkeley; the University of Newcastle, Australia; the University of Lund, Sweden; the University of Munich; the City University of Hong Kong; and The Hong Kong Polytechnic University. From 1996 to 1999 and 2001 to 2004, he served as the Head of the respective departments in Sydney and Hong Kong. His current research interests include control systems, complex networks, power systems, and stability analysis, especially in control and planning of future energy networks, basic stability, and control questions for dynamic networks.

Dr. Hill is a Fellow of the Society for Industrial and Applied Mathematics, USA, the Australian Academy of Science, the Australian Academy of Technological Sciences and Engineering, and the Hong Kong Academy of Engineering Sciences. He is also a Foreign Member of the Royal Swedish Academy of Engineering Sciences.